

Air-bridge microbolometer for far-infrared detection

Dean P. Neikirk and David B. Rutledge

Division of Engineering and Applied Science, California Institute of Technology, Pasadena, California 91125

(Received 22 August 1983; accepted for publication 24 October 1983)

A new microbolometer for far-infrared detection has been fabricated that allows an increase in sensitivity of a factor of 4 over the best previously reported bolometer. By suspending the detector in the air above its substrate a reduction in the thermal conductance out of the device by a factor of 5 has been achieved. At a modulation frequency of 100 kHz this microbolometer has an electrical noise equivalent power of $2.8 \times 10^{-11} \text{ W(Hz)}^{-1/2}$. A thermal model is also presented that accurately fits the response of the detector.

PACS numbers: 07.62. + s, 42.80.Qy, 44.10. + i, 85.40.Ek

In the millimeter and submillimeter region of the spectrum the use of integrated antennas and detectors is being applied more and more widely.¹⁻³ However, since the detectors used are much smaller than a wavelength they often require fairly sophisticated fabrication procedures. One relatively simple detector that provides sensitive video detection throughout this region is the bismuth microbolometer.⁴ This type of thermal detector achieves both high sensitivity and speed because of its physically small size: typically four micrometers square and one-tenth of a micrometer thick, fabricated on a quartz substrate using conventional photolithography and lift-off. In order to increase the sensitivity of the microbolometer we have developed a technique which allows the suspension of the device in the air above the substrate. This removes the major thermal conduction pathway out of the detector, providing a significant improvement in performance. We call this new device an air-bridge microbolometer.

The air-bridge bolometer is fabricated using a modified photoresist bridge technique.^{5,6} In the usual process the bridge is suspended above the substrate by another layer of flood exposed resist. In order to make an air-bridge bolometer three layers of resist are used, with only the middle layer flood exposed. When the trilayer resist is contact printed to form the bridge pattern an identical pattern is produced in the bottom layer. A finished photoresist structure is shown in Fig. 1. Electrical contacts for the microbolometer are then formed by evaporating 100 nm of silver at normal incidence to the substrate. Bismuth is then evaporated at a 50° angle from each side of the bridge. In this way 100 nm of bismuth is deposited under the bridge, but supported above the substrate by the bottom resist layer. After evaporation the substrate is soaked in acetone for approximately one hour, which dissolves all of the photoresist. Unwanted metal on the top layer of resist is removed, and the bolometer is left suspended by its ends above the substrate when the resist below it dissolves away (Fig. 2). For comparison, standard substrate-supported bolometers were also made by omitting the bottom layer of resist.

The thermal properties of the air-bridge bolometer can be modeled as a bar of material in which power is uniformly dissipated, and whose ends are connected to perfect heat sinks (the silver electrical contacts here). Calculating the temperature rise in the bolometer is then a simple one-dimensional heat flow problem. The thermal diffusion equa-

tion describing the complex temperature rise ϕ in the device is

$$\frac{\partial^2 \phi}{\partial x^2} = \frac{\rho C}{K} \frac{\partial \phi}{\partial t} - \frac{P_0}{2lAK} (1 + e^{i\omega t}), \quad (1)$$

where l is the length of the bolometer and A its cross-sectional area; ρ is the bolometer material density, C its specific heat, K its thermal conductivity, and P_0 the peak power dissipated. This equation is solved subject to the boundary condition that ϕ is zero at the ends of the device. The quantity of practical interest is the temperature rise averaged over the bolometer which is obtained by integrating the solution over x . We can then interpret the ratio of the time-varying temperature and time-varying power as a complex thermal impedance $Z_r(\omega)$, which is

$$Z_r(\omega) = 2 \frac{l}{AK} \left(\frac{L}{l} \right)^3 \left(\frac{l}{2L} - \tanh \frac{l}{2L} \right), \quad (2)$$

where L is the complex thermal diffusion length and $L = (K/i\omega\rho C)^{1/2}$. The bolometer responsivity is given by

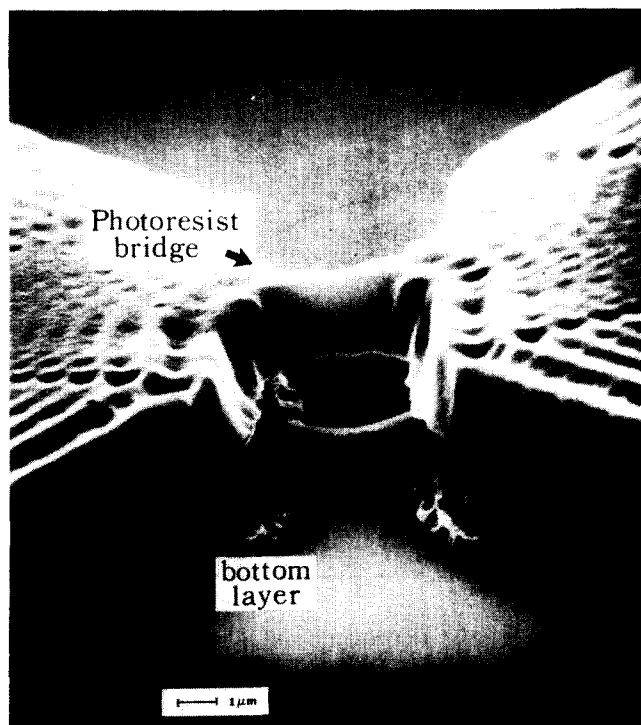


FIG. 1. Trilayer resist pattern used to make the air-bridge bolometers.

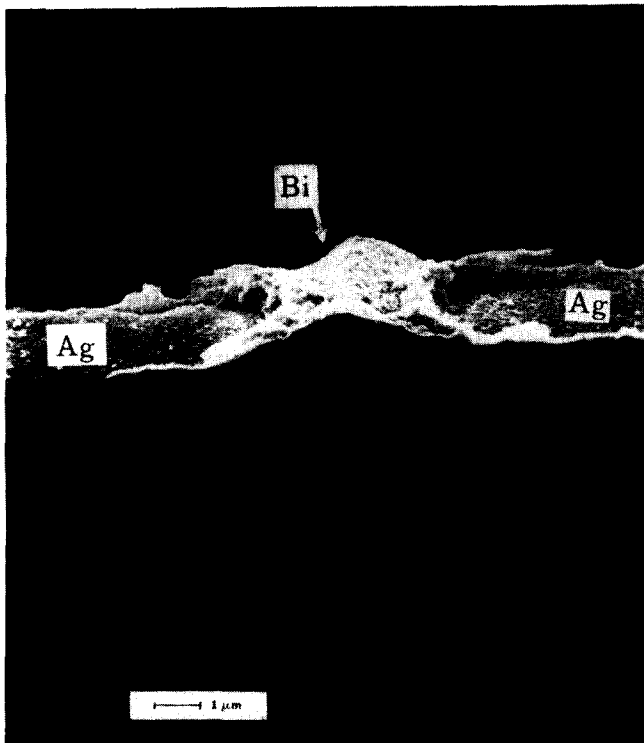


FIG. 2. Air-bridge bismuth microbolometer. The bolometer is $4 \mu\text{m}$ long from one silver connection to the other, $3.5 \mu\text{m}$ wide, and 100 nm thick.

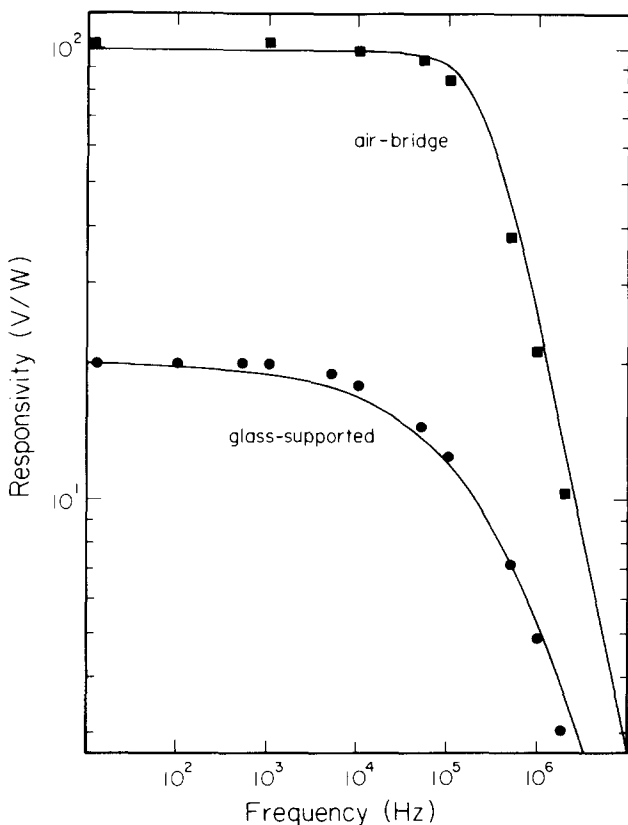


FIG. 3. Responsivity vs frequency for the air-bridge and substrate supported bolometers. The solid line for the air bridge is fitted from Eq. (2), for the glass-supported device fitted using Ref. 4. Both had a dc resistance of about 100Ω , and were biased to 0.1 V .

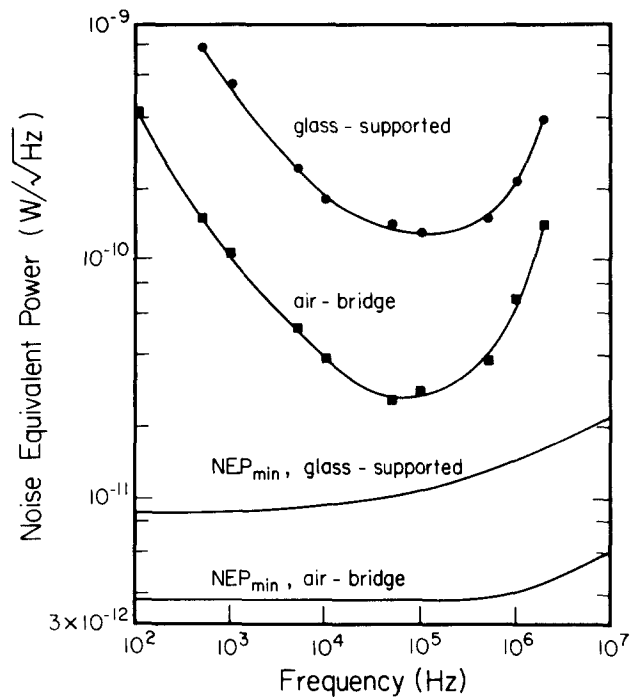


FIG. 4. Noise equivalent power for the detectors in Fig. 3. The noise was measured with a PAR 124 lock-in.

$R = \alpha |Z_t| V_b$, where α is the temperature coefficient of resistance for the bolometer material and V_b the dc bias voltage across the device. For low frequencies the thermal diffusion length L is greater than the device length l , and $Z_t = l / 12KA$, independent of frequency. At high frequencies where L is much smaller than l we find $Z_t = 1/i\omega\rho A l C$. These are just the limiting values for an equivalent thermal circuit consisting of a resistance $l / 12KA$ in parallel with a thermal capacitance $\rho A l C$. This predicts a frequency response that scales like $1/l^2$.

Figure 3 shows typical measured responsivities of both air-bridge and substrate-supported bolometers of the same size, along with fitted curves from Eq. (2). The dc value of the responsivity is found by measuring the bolometer I - V curve, and from this finding the resistance versus power curve for the device. For the input powers of interest (less than $500 \mu\text{W}$) the R - P curve is a straight line. The dc responsivity is the product of the slope of this line and the bias point current. The frequency response of the bolometer is then measured with an amplitude modulated 150-MHz source.⁵ Note that by suspending the bolometer above the substrate, the thermal impedance (inferred from the increase in responsivity) has increased by a factor of 5 over the standard device.

For the air-bridge bolometer all the physical constants and device dimensions in Eq. (2) are known, with the exception of the thermal conductivity of thin-film bismuth. Since both the electrical and thermal properties of bismuth films are strongly dependent on thickness and deposition conditions^{7,8} K is treated as an adjustable parameter in the fitted curve. It is directly obtained from the dc responsivity R_{dc} which gives $K = \alpha V_b l / 12 R_{dc} A$. In the curve shown $\alpha = -0.003 \text{ K}^{-1}$, $V_b = 0.1 \text{ V}$, $l/A = 11.5 \mu\text{m}^{-1}$, and $R_{dc} = 99 \text{ V/W}$, which gives a thermal conductivity of 2.9 W/mK . This value is about three times lower than that of bulk

bismuth, but twice the value for 100-nm-thick films given in Ref. 8. The excellent agreement between the fitted curve with this value of K and the measured responsivity at high frequency indicates that the simple thermal model used is valid for the air-bridge bolometer.

The noise spectra for these detectors have also been measured. For both detectors the noise decreased like $f^{-1/2}$ from about $40 \text{ nV}/\sqrt{\text{Hz}}$ at 100 Hz to $2 \text{ nV}/\sqrt{\text{Hz}}$ at 100 kHz (for a dc bias of 0.1 V across the devices). Above 100 kHz the noise is limited by Johnson noise only. Using these noise spectra and the responsivities from Fig. 3, the electrical noise equivalent power (NEP) can be calculated, and is shown in Fig. 4. The NEP below 50 kHz is limited by $1/f$ noise and above 100 kHz by the roll-off in the bolometer responsivity. Because of the reduced thermal conductance the air-bridge bolometer's NEP is over four times smaller than the substrate-supported device. Since the thermal impedance for these detectors is known, it is possible to calculate their thermal fluctuation limited NEP, which is also shown in Fig. 4. This is given by⁹ $[4kT^2 \text{Re}(1/Z_t)]^{1/2}$, which at 300 K is $3.8 \times 10^{-12} \text{ W(Hz)}^{-1/2}$ for the air bridge, and $8.6 \times 10^{-12} \text{ W(Hz)}^{-1/2}$ for the glass-supported detector. The measured air-bridge NEP at 100 kHz is only a factor of 8 from its fundamental limit, and a factor of 3.5 from the limit of a comparable glass-supported device.

In conclusion, we have demonstrated a new air-insulated microbolometer which provides a significant improve-

ment in performance over standard glass-supported bolometers. We have also found an accurate model for predicting how the thermal response of this device varies with its physical dimensions. The dc response scales like l/A and the roll-off frequency like $1/l^2$. With our minimum lithographic linewidth of $4 \mu\text{m}$ we have a 3-dB frequency of 400 kHz; by reducing linewidths to $1 \mu\text{m}$ this should increase to over 6 MHz with no decrease in dc response.

We would like to acknowledge the support of the Jet Propulsion Laboratory through Dr. M. Litvak, and the Department of Energy under contract DEAM03-765F-00010 Task 11A.

¹C. Yao, S. E. Schwarz, and B. J. Blumenstock, *IEEE Trans. Microwave Theory Tech.* **30**, 1241 (1982).

²B. J. Clifton, G. D. Alley, R. A. Murphy, and I. H. Mroczkowski, *IEEE Trans. Electron Devices* **28**, 155 (1981).

³D. P. Neikirk, D. B. Rutledge, M. S. Muha, H. Park, and C.-X. Yu, *Appl. Phys. Lett.* **40**, 203 (1982).

⁴T.-L. Hwang, S. E. Schwarz, and D. B. Rutledge, *Appl. Phys. Lett.* **34**, 773 (1979).

⁵D. P. Neikirk and D. B. Rutledge, *Appl. Phys. Lett.* **41**, 400 (1982).

⁶D. M. Dobkin and D. B. Cantos, *IEEE Electron Dev. Lett.* **EDL-2**, 222 (1981).

⁷A. Kawazu, Y. Saito, H. Asahi, and G. Tominaga, *Thin Solid Films* **37**, 261 (1976).

⁸V. Abrosimov, B. Egorov, and M. Krykin, *Zh. Eksp. Teor. Fiz.* **64**, 217 (1973) [*Sov. Phys. JETP* **37**, 113 (1973)].

⁹R. A. Smith, F. E. Jones, and R. P. Chasmar, *The Detection and Measurement of Infrared Radiation* (Oxford University, London, 1968), p. 221.

Transversely excited N₂O sequence band laser

Hiroshi Hara^{a)} and W. T. Whitney

Laser Physics Branch, Naval Research Laboratory, Washington, D. C. 20375

(Received 22 August 1983; accepted for publication 24 October 1983)

Sequence band operation of a transversely excited nitrous oxide laser is reported for the first time. The sequence laser could be tuned to each V - R line from $R(25)$ to $R(14)$ and from $P(14)$ to $P(26)$ in the $10.7\text{-}\mu\text{m}$ band. Output energies were $10 \mu\text{J}$ – 1 mJ . Improved stability of the discharge at high specific energy loading and use of an intracavity hot cell made sequence band oscillation possible.

PACS numbers: 42.55.Hq, 42.60.By

Sequence band (00^2 – 10^1) operation of the cw N₂O laser was first reported¹ in 1977, but to our knowledge, there has been no previous report of a pulsed transversely excited (TE) N₂O laser operating on the sequence band. A major impediment has been that transverse discharges containing N₂O are very susceptible to bright arc instabilities due to the relatively large electron attachment rates of gas mixtures containing N₂O.² This problem is particularly severe at the higher specific energy loadings required for sequence band oscillation as compared with regular band operation.³ In a recent publication,⁴ we have demonstrated that addition of a

small percentage of H₂ to the N₂O laser gas mixture effectively nullifies the electron attachment process, and allows stable discharges at high specific energy loadings to be obtained. Combining this technology with the use of a conventional intracavity hot cell⁵ has enabled us to obtain sequence band oscillation of the TE N₂O laser. These results make possible relatively high power laser radiation at the N₂O sequence band set of wavelengths in the $10\text{-}\mu\text{m}$ region.

The transverse discharge volume of our laser was $\sim 2 \times 2 \times 100 \text{ cm}^3$ between solid copper electrodes which had modified Rogowski profiles. Preionization of the discharge region was provided by a sliding-spark board located on one side of the electrodes, and fired $\sim 2 \mu\text{s}$ before the main discharge. Discharge energy was delivered from a triggered

^{a)} Permanent address: First Research Center, Japan Defense Agency, 2-2-1 Nakameguro, Meguro, Tokyo, 153 Japan.